

Neighborhood Consensus Contrastive Learning for Backward-Compatible Representation

Shengsen Wu^{1,*}, Liang Chen^{2,*}, Yihang Lou³, Yan Bai¹, Tao Bai³, Minghua Deng² and Lingyu Duan¹

¹ Institute of Digital Media, Peking University

² School of Mathematical Sciences, Peking University

³GoTen AI Lab, Intelligent Vision DeptHuawei Technologies

Abstract

In object re-identification (ReID), the development of deep learning techniques often involves model update and deployment. It is unbearable to re-extract image features of the large-scale gallery when deploying new models. Therefore, backward-compatible representation is proposed to enable the “new” features compatible with “old” features, free from the re-extracting process. The existing backward-compatible methods simply conduct constraints in the embedding space or discriminative space and ignore the intra-class variance of the old embeddings, resulting in a risk of damaging the discriminability of new embeddings.

In this work, we propose a Neighborhood Consensus Contrastive Learning (NCCL) method, which learns backward-compatible representation from a neighborhood consensus perspective with both embedding structures and discriminative knowledge. With NCCL, the new embeddings are aligned and improved with old embeddings in a multi-cluster view. Besides, we also propose a scheme to filter the old embeddings with low credibility, which can further improve the compatibility robustness. Our method ensures backward compatibility without impairing the accuracy of the new model. And it can even improve the new model’s accuracy in most scenarios.

1. Introduction

General object re-identification (ReID) aims at finding a significant person/vehicle of interest in a large amount of collection, called “gallery”. It has attracted much interest in computer vision due to its great contributions in urban surveillance and intelligent transportation [41, 20]. Specifically, existing ReID methods typically map each image into vector space using a convolutional neural network. The output in vector space is usually called “embedding”. Given

query images, the process of ReID is to identify their nearest neighbors in the gallery by measuring distance with respect to their embeddings.

As the new training data or the improved model designs are available, the deployed model will be updated to a new version with better performance. Then we need to re-process the images in the gallery to harvest the benefits of the new model, namely “backfilling”. However, it is common to have millions or even billions of images in the database/gallery [29], which makes backfilling a painful process. An ideal solution is enabling “new” embeddings to be compared with “old” embeddings directly so that new models can be deployed without backfilling.

To achieve backfilling-free, the backward-compatible representation learning methods have recently arisen. Under backward-compatible setting, given an anchor sample from new embeddings, no matter the positives and negatives from old/new embeddings, the anchor is consistently closer to the positives than the negatives. Recently, Budnik *et al.* [3] adopt metric learning methods to optimize the distances between new and old embeddings in an asymmetric way. However, the adopted pair-based triplet losses can not well consider the feature cluster structure differences across different embeddings. Such less informative optimization and redundant sampling is hard to apply on large-scale dataset. Alternatively, Shen *et al.* [30] use the classifier of the old model to regularize the new embeddings in training the new model, termed as “backward-compatible training (BCT)”. The old classifier is based on a weight matrix, where each column corresponds to a particular class in old training sets. Therefore, BCT can only work when the new and old training sets have common classes.

The old embedding space is often not ideal and faces complicated cluster structures. For example, due to the intra-class variance caused by varied postures, colors, viewpoints, and lighting conditions, the cluster structure often tends to be scattered as multiple sub-clusters. Moreover, the old embedding space also inevitably contains some noise data and outliers in clusters. Simply constraining the

This work is completed in Huawei Co.Ltd. * means the equal contribution.

learned “anchor” of new embeddings close to the randomly sampled “fixed positives” of old embeddings has a risk of damaging the discriminability of new embeddings. Therefore, it is necessary to consider the entire cluster structure across new and old embeddings in backward-compatible learning.

In this work, we propose a Neighborhood Consensus Contrastive Learning (NCCL) method for backward-compatible representation. Specifically, we design a supervised contrastive learning loss to optimize the distances between the new and old features by a cluster view. The different samples within a cluster are attentively considered by a neighborhood consensus scheme. Accordingly, the new embeddings gather with the corresponding old clusters with high priority. Typically, the classifier head in a network converts the embedding space to discrimination space for classification. Therefore, the discriminative space contains rich class-level information [46]. Correspondingly, we further design a soft pseudo-multi-label task to exploit such knowledge to enhance the backward-compatible learning. Such task is also an auxiliary apart from the new models’ original classification task, making the new embeddings more discriminative.

Besides, the old model may produce poor embeddings with newly added training data. Achieving compatibility with poor old embeddings does not contribute to backward-compatible learning but impair the performance of the new models. Therefore, we combine the mixture Gaussian kernel model and entropy criterion to remove the old embeddings with low credibility. It helps to maintain robustness when learning backward-compatible representation from old models with various qualities.

The contributions of this paper are summarized as follows:

- We propose a Neighborhood Consensus Contrastive Learning (NCCL) method for backward-compatible representation. The NCCL exploits the neighborhood structure in both the embedding and discrimination spaces.
- We propose a novel scheme to filter the old embeddings with low credibility, which is helpful to improve the robustness against the noise data in old models.
- The proposed method obtains state-of-the-art performance on the evaluated benchmark datasets. We can ensure backward compatibility without impairing the accuracy of the new model.

2. Related work

2.1. Object re-identification

Object re-identification technology is widely used in target tracking and intelligent security, mainly including person re-identification and vehicle re-identification. It can

realize cross-camera image retrieval, tracking, and trajectory prediction of pedestrians or vehicles. In recent years, driven by deep learning technology, research in the object re-identification field has mainly focused on network architecture design [34, 50, 28], feature representation learning [44, 39], deep metric learning [37, 5, 14, 48], ranking optimization [40, 1], and recognition under video sequences [18, 12, 22]. This paper is to learn backward-compatible representation for ReID models.

2.2. Backward-compatible representation

Backward-compatible learning, also called “asymmetric learning”, encourages the new embeddings closer to the old embeddings with the same class ID than that with different class IDs. It is an emerging topic. To the best of our knowledge, there only exist two pieces of research. Budnik *et al.* [3] proposes an asymmetric metric learning paradigm. We call this method Asymmetric for convenience. It provides a perspective: we can regard new embeddings as “anchor” and old embeddings as “positives/negatives” to achieve backward-compatible learning by metric learning losses. Shen *et al.* [30] proposes BCT, a backward-compatible representation learning model. BCT feeds the new embeddings into the old classifier. Then the output logits are optimized with cross-entropy loss. BCT and Asymmetric are essentially identical, as it is equivalent to a smoothed triplet loss where each old embedding class has a single center [27]. With the newly added data, BCT needs to use knowledge distillation techniques. In general, existing methods simply conduct constraints in the embedding space or discriminative space and ignore the intra-class variance of the old embeddings. In this article, we consider this problem from a neighborhood consensus perspective with both embedding structure and discriminative knowledge.

2.3. Contrastive learning

Self-supervised learning uses the characteristics of the data to construct supervision signals to assist downstream tasks [24]. In recent years, it has been sought after by many researchers in the fields of computer vision and natural language processing. Contrastive learning is a typical type of self-supervised learning. It learns representations by contrasting positive pairs against negative pairs. Many state-of-the-arts methods for unsupervised representation learning tasks are based on contrastive learning [15, 6]. There are instance-based [8, 7, 13], cluster-based [4, 23], mixed instance and cluster-based contrastive learning methods [33, 47]. Although data augmentation can supply positive samples, one potential deviation of the unsupervised contrastive learning method is that negative samples may be noisy [9]. Therefore, some researchers have proposed supervised contrastive learning [21] and semi-supervised con-

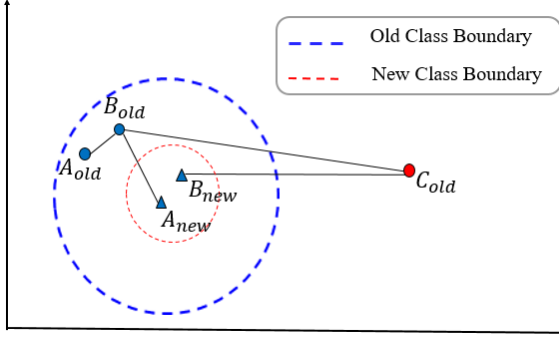


Figure 1. Pairwise distance relationship in the feature space. A and B come from the same class, while C belongs to other classes.

trastive learning algorithms [19]. In this article, we design a neighborhood consensus supervised contrastive learning method to achieve the compatibility of new and old features.

3. Methods

3.1. Problem formulation

Following the formulation in [30], a ReID model contains two modules: an embedding function $\phi : \mathcal{X} \rightarrow \mathcal{Z}$ that lifts any query image $x \in \mathcal{X}$ into vector space \mathcal{Z} and a classifier $\varphi : \mathcal{Z} \rightarrow \mathcal{R}^K$.

Assume that we have an old embedding function ϕ_{old} that is trained on the old training dataset \mathcal{D}_{old} with K_{old} IDs. Then we have a new embedding function ϕ_{new} and a new classifier φ_{new} trained on the new training data \mathcal{D}_{new} with K_{new} IDs. \mathcal{D}_{new} can be a superset of \mathcal{D}_{old} . The label space is set to \mathcal{Y} .

We define the gallery set as \mathcal{G} , and the embeddings of images in \mathcal{G} are obtained by ϕ_{old} . The query images are transformed to embeddings by ϕ_{old} in the test stage. Assume that M is a metric, e.g., mAP or top- k accuracy, to evaluate the effectiveness of the retrieval between the gallery set and the query set, then $M(\phi_{old}, \phi_{old})$ is the self-test result using the old embedding model. Once the ReID system is updated, similarly, $M(\phi_{new}, \phi_{new})$ is the self-test result based on the ϕ_{new} for both gallery and query. Since the number of images in \mathcal{G} could be extremely large, it is costly to refresh the embeddings in \mathcal{G} . Therefore, $M(\phi_{new}, \phi_{old})$ refers to the cross-test result using ϕ_{new} for query and ϕ_{old} for the gallery. Empirically, the goal of backward-compatible learning is to accomplish $M(\phi_{new}, \phi_{new}) \geq M(\phi_{new}, \phi_{old}) \geq M(\phi_{old}, \phi_{old})$.

3.2. Backward-compatible criterion

Shen *et al.* [30] give a strict criterion of backward-compatible compatibility in BCT.

$$d(\phi_{new}(x_i), \phi_{old}(x_j)) \geq d(\phi_{old}(x_i), \phi_{old}(x_j)), \quad \forall (i, j) \in \{(i, j) : y_i \neq y_j\}. \quad (1)$$

$$d(\phi_{new}(x_i), \phi_{old}(x_j)) \leq d(\phi_{old}(x_i), \phi_{old}(x_j)), \quad \forall (i, j) \in \{(i, j) : y_i = y_j\}. \quad (2)$$

Such definition may lead to the increase of variance in the new embedding classes in some cases. As shown in Figure 1, the new embeddings A_{new} and B_{new} are obviously backward-compatible with their old embeddings. However, we can find $d(B_{new}, C_{old}) < d(B_{old}, C_{old})$ and $d(A_{new}, B_{old}) > d(A_{old}, B_{old})$, which do not satisfy Eq. 1 and 2. Constraining A_{new} and B_{new} to satisfy the inequality will lead to sub-optimal solutions.

Therefore, we come up with a new backward-compatible criterion:

$$d(\phi_{new}(x_i), \phi_{old}(x_j)) < d(\phi_{new}(x_i), \phi_{old}(x_k)), \quad \forall (i, j, k) \in \{(i, j, k) : y_i = y_j \neq y_k\}. \quad (3)$$

The triplet constraint in (3) precisely describes the relationship between the new and old models when they are backward-compatible. Given a image x_i , the distance between the new embedding $\phi_{new}(x_i)$ (anchor) and other old embeddings $\phi_{old}(x_j)$ (fixed positives) is smaller than the distance between it and the embeddings $\phi_{old}(x_k)$ (fixed negatives).

3.3. Neighborhood consensus supervised contrastive learning

To satisfy the inequality (Eq. 3), a straightforward solution is to adopt the metric learning loss in an asymmetric way, e.g., triplet loss [3], cross-entropy [30]. However, It has several limitations: 1) The potential manifold structure of the data can not be characterized by random sampling instances or classifiers [27]. 2) They are susceptible to those boundary points or outliers with the newly added data, making the training results unpredictable. 3) They treat all the old embeddings equally important, which can be overwhelmed by less informative pairs, resulting in inferior performance [32].

In this work, we propose a neighborhood consensus supervised contrastive loss with multiple positives and negatives to exploit the neighborhood structural information. The InfoNCE based contrastive loss [25] is commonly used for self-supervised learning, proving that its contrastive power increases with more positives and negatives. To flexibly select neighborhood, memory banks [38] are adopted to store the fixed positives/negatives, termed as \mathcal{B} . It can represent the potential manifold structural information of the old embedding space.

Here the neighborhood consensus weight is introduced to measure the affinity relationship between anchors and fixed positives. Ideally, each new anchor embedding should focus on the fixed positives from its corresponding old embedding cluster. However, the boundaries between local clusters may be blurred. Thus we adopt the soft weight to

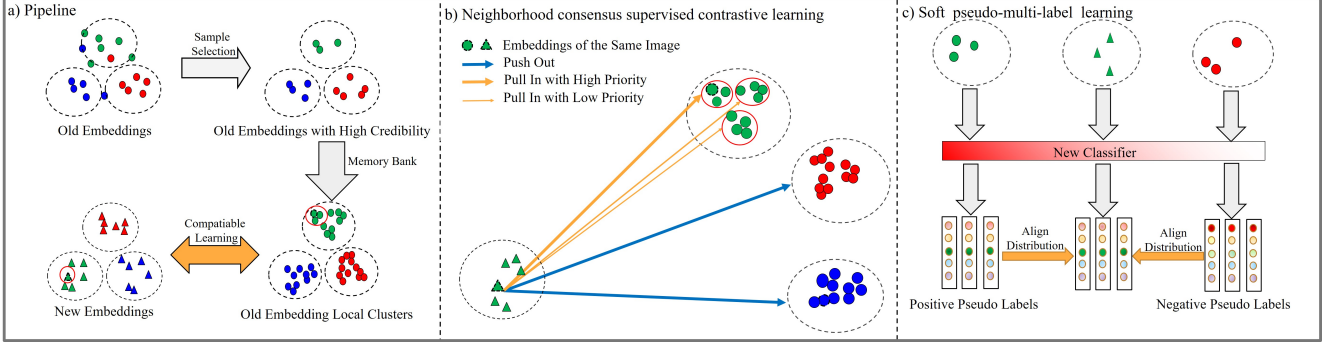


Figure 2. An illustration of our method NCCL. The left part shows the highly credible sample selection and contrastive learning in the embedding space; The middle part shows that each anchor gives different attention weights for different positives; The right part shows that the pseudo-multi-labels are used to align the discriminative distribution.

concentrate more on the positives which are more informative. “More informative” means higher probability to belong to a local cluster corresponding to the anchor. Given a positive image pair (x_i, x_p) and view x_i as the anchor, it is intuitive that the weight w_{ip} of $\phi_{old}(x_p)$ rises in inverse proportion to the distance between $\phi_{old}(x_i)$ and $\phi_{old}(x_p)$. Specifically, we calculate the soft neighborhood consensus weight based on the cosine distance, regarded as the prior knowledge and given by

$$w_{ip} = \frac{1}{2} \left(\frac{\phi_{old}(x_i)\phi_{old}(x_p)}{\|\phi_{old}(x_i)\|\|\phi_{old}(x_p)\|} + 1 \right) \in [0, 1]. \quad (4)$$

Define $A(i) \equiv \mathcal{B} \setminus \{i\}$ and $P(i) \equiv \{p \in A(i) : y_p = y_i\}$, our training objective on the embedding space is a weighted generalization of contrastive loss, given by

$$L_1 = \sum_{i \in \mathcal{D}_{new}} \sum_{p \in P(i)} -w_{ip} \log s_{ip}. \quad (5)$$

Where the s_{ip} represents the affinity score of positive p contrasted with anchor i , written as

$$s_{ip} = \frac{\exp(\phi_{new}(x_i)\phi_{old}(x_p)/\tau)}{\sum_{a \in A(i)} \exp(\phi_{new}(x_i)\phi_{old}(x_a)/\tau)}. \quad (6)$$

Where τ is a temperature parameter that controls the sharpness of similarity distribution. Minimizing L_1 is equivalent to maximize the affinity scores between anchors and positives. The existence of weight forces the optimized gradient direction to be more biased towards those positive pairs that are geometrically closer. Therefore, the neighborhood consensus contrastive learning procedure on the embedding space actually ensures the alignment of the old and new embeddings at the granularity of local clusters.

3.4. Soft pseudo-multi-label learning on the discriminative space

As the embedding space represents the instance-level knowledge, the proposed neighborhood consensus supervised contrastive learning can be regarded as an intra-class

alignment between old and new embeddings. While the discriminative space represents the class-level knowledge, which defines the probability distribution of each sample belonging to underlying class centers on the simplex [43]. Intuitively, we can impose constraints on classifiers to achieve the class-level alignment and furthermore, tightening.

With the new classifier, we construct a pseudo-multi-label learning task from a different perspective than semantic-level label learning. Specifically, given an image x_i , its positive image set P and negative image set N , we compare the discrimination vector $\varphi_{new}(\phi_{new}(x_i))$ with discrimination vector set $\{\varphi_{new}(\phi_{old}(x_p)), x_p \in P\}$ and $\{\varphi_{new}(\phi_{old}(x_n)), x_n \in N\}$. Intuitively, $\varphi_{new}(\phi_{new}(x_i))$ should be similar to any positive discrimination vector $\varphi_{new}(\phi_{old}(x_p))$ and dissimilar to any negative discrimination vector $\varphi_{new}(\phi_{old}(x_n))$. Thus, the positive/negative discrimination vectors can be regard as pseudo-multi-labels as a supplement to ground truth. As the ground truth may only reflect a single facet of the complete knowledge encapsulated in real world data, the proposed pseudo-multi-label is an auxiliary apart to mine richer knowledge, resulting in the new embeddings with better performance. Here we imitate the contrastive procedure in the embedding space for harmonization. A memory bank is also utilized to store the positive/negative discriminative vector. We give the dual soft contrastive loss on the discriminative space below,

$$L_2 = \sum_{i \in \mathcal{D}_{new}} \sum_{p \in P(i)} -w_{ip} \log \tilde{s}_{ip}, \quad (7)$$

$$\tilde{s}_{ip} = \frac{\exp(\varphi_{new}(\phi_{new}(x_i))\varphi_{new}(\phi_{old}(x_p))/\tau)}{\sum_{a \in A(i)} \exp(\varphi_{new}(\phi_{new}(x_i))\varphi_{new}(\phi_{old}(x_a))/\tau)}. \quad (8)$$

Where the weight w_{ip} is the same as in equation (4).

Discussion. If we only use the semantic-label guided cross-entropy loss to optimize the new and old discriminative probabilities of images, it ensures that these two prob-

ability vectors from the same sample fall in the same hyperplane block. Nevertheless, their distance on the simplex space cannot be guaranteed to be small since the final convergent probability vectors often do not tend to the ideal one-hot form, especially in a large amount of IDs scenario. Similarly, if we penalize the KL divergence of these two probability vectors, the ideal convergence state is that they are consistent. However, the divergence or variance of the discriminative distribution for each class may still be large. To better compress the variance, we jump out of the comparison of discriminative probabilities in a single sample and use the discriminative vectors of other samples with the same ID in the neighborhoods to constrain each other. Once the discriminative distribution divergence is reduced, the class structure would become compact.

3.5. Highly credible sample detection

Due to the variations of object morphology, illumination, and camera view in the Re-ID dataset, the intra-class variance of old embedding embeddings can be huge [2]. Poor old embeddings are often located in the fuzzy region between classes. Backward-compatible learning with such outlier samples would affect the retrieval accuracy of the new model.

Here, we introduce entropy to measure the uncertainty of sample classification. The greater the entropy, the smaller the credibility. Since the old classifier is not available, we construct the pseudo classification vectors $\tilde{p}(x)$ by calculating the allocation score of each sample belonging to old class centers. Specifically, suppose the $\hat{\mu}_k = \frac{1}{|\{i: y_i=k\}|} \sum_{y_i=k} \phi_{old}(x_i)$ is the k -th ($1 \leq k \leq K_{new}$) old class center. Then we utilize multiple Gaussian kernel functions to obtain the similarity score between samples and centers,

$$\tilde{p}(x_i)_k = \frac{\exp(-\frac{\|\phi_{old}(x_i) - \hat{\mu}_k\|^2}{\hat{\sigma}_k})}{\sum_{j=1}^{K_{new}} \exp(-\frac{\|\phi_{old}(x_i) - \hat{\mu}_j\|^2}{\hat{\sigma}_j})}. \quad (9)$$

Where $\hat{\sigma}_k$ represents the variance of k -th distance set $\{\|\phi_{old}(x_i) - \hat{\mu}_k\|^2 : y_i = k\}$. Then the uncertainty of i -th sample is the entropy of $\tilde{p}(x_i)$, namely $\mathcal{H}(x_i) = -\sum_{k=1}^{K_{new}} \tilde{p}(x_i)_k \log \tilde{p}(x_i)_k$. Since $\log K_{new}$ is the maximum value of \mathcal{H} , the uncertainty threshold boundary is set as \hat{U} which is related to $\log K_{new}$. Then we remove those samples with entropy larger than \hat{U} , and they do not participate in the soft supervised contrastive learning procedure.

Overall loss function. Combining with classification loss L_{new} on the new model trained independently, we give the final objective below,

$$L_{total} = L_{new} + \alpha L_1 + \beta L_2. \quad (10)$$

Where the α and β are two hyperparameters to control the relative importance of embedding space learning and discriminative space learning, respectively. Specifically, we

first use L_{new} and L_1 loss to train the entire new model. Then we freeze the weight of the classification head before adding the L_2 loss in training to avoid drastic changes in the old discriminative features. This step also actually helps stabilize the training of pseudo-multi-label learning.

4. Experiments

We evaluate our proposed method on two widely-used person ReID datasets, *i.e.*, Market-1501 [45], MSMT17 [36], and one vehicle ReID dataset VeRi-776 [35]. We first implement several baselines, and then test the potential of our method by applying it to the case of multi-factor changes, including model changes and loss changes. We also conduct a multi-model test to evaluate the sequential compatibility. Besides, we adopt the large-scale ImageNet [10] and Place365 [49] datasets to demonstrate the scalability of our method.

4.1. Datasets and evaluation metrics

Market1501 consists of 32,668 annotated images of 1,501 identities shot from 6 cameras in total. MSMT17 is a large-scale ReID dataset consisting of 126,441 bounding boxes of 4,101 identities taken by 15 cameras. VeRi-776 contains over 50,000 images of 776 vehicles captured by 20 cameras covering a 1.0 km^2 area in 24 hours. ImageNet contains more than 1.2 million images with 1,000 classes. Place365 has about 1.8 million images with 365 classes. For ImageNet and Place365, we conduct the retrieval process on the validation sets of these two datasets, *i.e.*, each image will be taken as a query image, and other images will be regarded as gallery images.

Mean average precision (mAP) and top- k accuracy are adopted to evaluate the performances of retrieval. The self-test performance and cross-test performance are used to evaluate the performances of backward-compatible representation. Self-test means that ϕ_{new} is used to extract embeddings for both the query set and the gallery set. Cross-test means that ϕ_{new} is used to extract embeddings for the query set while ϕ_{old} is used to compute embeddings for the gallery set.

4.2. Implementation details

We use 4 NVIDIA Tesla V100 GPUs for training. The input size of the models is set to 384×128 pixels. The implementations of all compared methods, including L_2 regression, BCT, Asymmetric, and our NCCL, are based on the FastReID [17]. The default configuration of FastReID is adopted, including weight decay, learning rate, etc. The parameters α , β , and τ are taken as 0.01, 0.01, 1.0 by default, respectively. We set $\hat{U} = \frac{\log K_{new}}{2}$ as the default credible sample selection threshold. Without additional explanation, we use ResNet-18 [16] as the backbone to obtain a 512-dimensional embedding feature vector and cross-entropy as

Table 1. Performance comparison on Market1501, MSMT17 and VeRi-776 datasets.

Methods	Market1501				MSMT17				VeRi-776			
	Self-Test		Cross-Test		Self-Test		Cross-Test		Self-Test		Cross-Test	
	R1	mAP										
Ori-Old(R18)	82.96	63.26	-	-	57.02	29.24	-	-	89.35	56.91	-	-
L_2 loss	91.66	78.69	3.03	2.27	67.3	39.57	0.51	0.26	91.13	63.75	4.23	2.97
BCT[30]	91.69	77.47	84.74	66.86	67.91	39.11	58.18	30.44	92.02	64	80.86	56.41
Asymmetric[3]	91.98	81.08	85.45	68.4	71.95	45.29	53.9	28.15	91.26	66.59	81.01	56.28
NCCL(Ours)	92.87	81.9	85.51	69.15	73.43	46	59.64	30.92	92.62	70.15	81.37	58.82
Ori-New(R18)	92.37	80.84	22.71	13.81	70.52	42.86	10.06	4.11	92.26	67.21	19.7	10
Ori-Old(R50)	87.23	70.48	-	-	64.29	36.45	-	-	91.9	62.91	-	-
L_2 loss	93.97	84.31	47.3	28.97	72.43	47.16	30.91	13.22	93.15	70.61	47.5	25.64
BCT[30]	93.35	82.51	90.5	75.21	71.25	45.07	68.77	40.45	92.02	67.49	88.44	64.89
Asymmetric[3]	94.39	86.42	90.32	77.34	75.37	51.44	70.43	41.68	92.27	70.19	89.7	63.41
NCCL(Ours)	94.8	87.24	91.6	77.69	80.55	55.97	71.45	42.87	94.4	75.42	89.4	66.74
Ori-New(R50)	94.3	85.1	81.98	60.78	73.58	48.42	52.46	26.47	93.69	70.7	65.48	37.9

L_{new} . In our NCCL, the soft pseudo-multi-label learning only works in the later training stage, with the classifier froze.

4.3. Baseline comparisons

In this section, we conduct several baseline approaches for backward-compatible learning with backbone ResNet-18 and ResNet-50. With the same model architectures and loss functions, We set the old training data of 50% IDs subset and the new training data of 100% IDs complete set. The results on the three ReID datasets are shown in Table 1.

No regularization between ϕ_{new} and ϕ_{old} . We denote new model trained without any regularization as ϕ_{new*} . A simple case directly performs a cross-test between ϕ_{new*} and ϕ_{old} . As is shown in Table 1, backward compatibility is achieved at a certain degree. However, the cross-test accuracy fluctuates dramatically with the change of data set and network architecture, which is not enough to satisfy our backward-compatibility criterion. Subsequent experimental results will further confirm this opinion.

L_2 -regression between ϕ_{new} and ϕ_{old} output embeddings. An intuitive idea to achieve backward-compatibility is using L_2 loss to minimize the output embeddings’s euclidean distance between ϕ_{new} and ϕ_{old} , which was discussed in [30]. Such a simple baseline could not meet the requirement of backward-compatibility learning. The possible reason for L_2 loss failure is that L_2 loss is too local and restrictive. As it only focuses on decreasing distance between feature pairs from the same image, it ignores the distance restriction between negative pairs.

Asymmetric. It works better on small datasets than on large-scale datasets, probably owing to its inadequacy in utilizing the data intrinsic structure. For instance, Asymmetric’s cross-test outperforms the old model’s self-test on Market1501, but not on two VeRi-776, as is shown in 1.

BCT. As is shown in Table 1, BCT underperforms ϕ_{new*} in all self-test cases. The most likely reason is that BCT use synthesized classifier weights or knowledge distillation to deal with the newly added data. Synthesized clas-

Table 2. Performance comparison between different models on Market1501. The old model uses ResNet-18 with 50% training data. “mAP1” and “mAP2” represent the mean average precision of self-test and cross-test, respectively.

Methods	ResNet18-Ibn		ResNet50		ResNeSt50	
	mAP1	mAP2	mAP1	mAP2	mAP1	mAP2
Ori-Old	63.26	-	63.36	-	63.26	-
L_2 loss	80.05	1.19	84.54	0.56	83.03	0.59
BCT	78.92	66.70	82.03	68.65	86.64	68.76
Asymmetric	82.23	68.54	83.96	67.31	87.81	68.76
NCCL(Ours)	83.23	69.12	85.91	69.26	88.31	68.94
Ori-New	81.59	5.12	84.88	0.20	88.21	0.20

sifier weights for the newly added data are susceptible to those boundary points or outliers, making the training results unpredictable. Knowledge distillation assumes that the teacher model (old model) outperforms the student model (new model), which is not true in the application scenario of backward-compatible representation. As a result, it impairs the performance of the new model.

NCCL(Ours) with better self-test accuracy. As the effective utilization of the intrinsic structure, our approach fulfills the requirement of backward-compatible training and outperforms all compared methods. Besides, NCCL significantly outperforms ϕ_{new*} in all self-test cases. With the proposed method, the new embeddings could be improved with the old model’s information.

4.4. Changes in network architectures and loss functions

Here we study whether each method can be stably applied to various model architecture changes and loss function changes.

Model Changes. We first test the new model on ResNet18-Ibn, ResNet-50 and ResNeSt-50[42] instead of the old model ResNet-18 under the same loss function. ResNet18-Ibn only changes the normalization method of the backbone from batch normalization to instance batch normalization [26], and it keeps the structure consistent. It can be seen as a slight modification to the old model. ResNet-50 is composed of the same components with dif-

Table 3. Performance comparison between different losses on Market1501. The old model uses ResNet-18 with 50% training data. ‘‘mAP1’’ and ‘‘mAP2’’ represent the mean average precision of self-test and cross-test, respectively.

Methods	CircleSoftmax		ArcSoftmax		Softmax+Triplet	
	mAP1	mAP2	mAP1	mAP2	mAP1	mAP2
Ori-Old	63.26	-	63.36	-	63.26	-
L_2 loss	62.67	3.29	54.03	0.85	81.27	23.53
BCT	67.63	53.20	63.49	39.96	79.62	67.43
Asymmetric	67.27	28.77	56.71	5.09	81.75	68.07
NCCL(Ours)	79.62	49.28	71.06	31.38	82.36	69.15
Ori-New	78.96	3.69	67.31	0.93	81.55	14.20

ferent capacities compared to ResNet-18, which can be regarded as a middle modification to the old model. ResNeSt-50 introduces the split attention module into ResNet50, which makes it the most different from ResNet18. Note that the dimension of the feature vector in ResNet-50 and ResNeSt-50 is 2048, we will not directly feed the old feature with dimension 512 to ϕ_{new} but use the zero-padding method to expand the old feature to 2048-dimension.

As shown in Table 2, the comparison between independently trained new models and old models is an epic failure. BCT, Asymmetric, and our proposed method have learned backward-compatibility representation. Besides, our approach remains the the-state-of-art and is more robust to model changes.

Loss Changes. Then we change the Softmax based loss function L_{new} to ‘‘ArcSoftmax’’ [11], ‘‘CircleSoftmax’’ [31] and ‘‘Softmax + Triplet’’ in the new model. CircleSoftmax and ArcSoftmax are both used in the classification head, and Triplet is used in the embedding head.

As shown in Table 3, the performances of various methods are consistent with the baseline under the change of embedding loss. In contrast, all methods have a significant decline in self-test and cross-test under classification loss changes. The possible reason is that classification loss in the new models determines the class structure, while the embedding loss tightens the sample’s representation. Among these methods, Asymmetric fails in both self-test and cross-test. BCT achieves slightly better performance in cross-test but significantly reduces new models’ performance, making it unnecessary to deploy new models. Our method can improve the performance of the new model stably while ensuring the performance of the cross-test.

4.5. No overlap between \mathcal{D}_{old} and \mathcal{D}_{new}

Old training data and classifiers are not available in many industry settings. For example, a model deployed as a black-box API takes images as input and returns the processed features, but the model’s parameters are not accessible. Besides, its classifier and training details are not available, neither does the formula of the loss function. This kind of setting is quite common when one department cooperates with the other.

In the previous experiments, we always assume that the

Table 4. Performance comparison of no overlap between \mathcal{D}_{old} (25% IDs) and \mathcal{D}_{new} (75% IDs) on Market1501.

Methods	Self-Test			Cross-Test		
	R1	R5	mAP	R1	R5	mAP
Ori-Old	70.13	86.07	46.42	-	-	-
L_2 loss	90.29	96.32	76.24	15.86	35.33	9.41
BCT	86.73	94.86	69.60	62.29	83.49	41.63
Asymmetric	91.03	96.67	78.91	74.55	90.23	53.07
NCCL(Ours)	92.22	97.09	80.88	77.73	90.94	55.91
Ori-New	90.17	96.32	77.52	6.00	16.60	3.92

\mathcal{D}_{new} is a superset of \mathcal{D}_{old} . Here we investigate whether no overlap between them could sharply affect the compatibility performance of each method. The old model is trained with the randomly sampled 25% IDs subset of training data in the Market1501 dataset, and the new model is trained with the other 75% IDs subset. We show the results in Table 4.

Compared with baseline, the accuracy of all evaluated methods has dropped except for NCCL. The performance degradation of BCT is the most severe because it can only use synthesized classifier weights or knowledge utilization in this case[30]. Both of them can be regarded as a kind of knowledge distillation. As the old model is not good enough, it is intuitive to obtain unsatisfactory results when distilling knowledge from such model.

Our method does not require the old classifier, and the processing method for overlapping and non-overlapping training data is consistent. As we use sample selection and neighbor relationship maintenance, our method achieves the same effect as the baseline in this case.

4.6. Multi-model and sequential compatibility

Here we investigate the sequential compatibility case of multi-model. The first model ϕ_1 is trained with the randomly sampled 25% IDs subset of training data in the Market1501 dataset, and the second model ϕ_2 is trained with a 50% subset. Finally, the third model ϕ_3 is trained with the full dataset. We train ϕ_2 using backward-compatible methods with ϕ_1 and train ϕ_3 using backward-compatible methods with ϕ_2 . Therefore, ϕ_3 has no direct influence on ϕ_1 . The results of the sequential compatibility test are shown in Table 5.

We observe that, by training with NCCL, the last model ϕ_3 is transitively compatible with ϕ_1 even though ϕ_1 is not directly involved in training ϕ_3 . It shows that transitive compatibility between multiple models is achievable through our method, enabling a sequential update of models. It is worth mentioning that our method still has significant advantages over other methods in cross-model comparison $\phi_3 \phi_1$.

4.7. Test on other two large-scale image datasets

As the need for backward-compatible learning stems from the fact that the gallery is too large to re-extract new embeddings, we also utilize large-scale ImageNet and Place365 datasets for training and evaluating each method.

Table 5. Performance comparison in sequential multi-modal experiment on Market1501. We train three models ϕ_1 (ResNet18+25% IDs), ϕ_2 (ResNet18+50% IDs) and ϕ_3 (ResNet18+100% IDs).

Methods	Market1501 (mAP)					
	(ϕ_1, ϕ_1)	(ϕ_2, ϕ_1)	(ϕ_2, ϕ_2)	(ϕ_3, ϕ_2)	(ϕ_3, ϕ_3)	(ϕ_3, ϕ_1)
Ori	46.42	7.49	63.30	14.15	80.85	5.62
L_2 loss	-	24.01	61.87	16.15	78.39	1.47
BCT	-	45.78	60.29	65.45	77.07	45.20
Asymmetric	-	45.68	62.88	67.51	81.28	48.85
NCCL(Ours)	-	45.89	64.27	69.76	82.28	52.76

Table 6. Performance comparison on two large-scale datasets, ImageNet and Place365. The new model uses ResNet-18 with 50% Data, while the new model uses ResNet-50 with 100% Data.

Methods	Place365				ImageNet			
	Self-Test		Cross-Test		Self-Test		Cross-Test	
	Top-1	Top-5	Top-1	Top-5	Top-1	Top-5	Top-1	Top-5
Ori-Old	27.0	55.9	-	-	39.5	60.0	-	-
BCT	32.7	62.2	27.6	57.6	41.9	65.3	42.2	65.5
Asymmetric	31.2	60.9	28.6	58.1	41.8	65.1	42.9	63.3
NCCL(Ours)	35.1	64.1	28.7	58.1	62.5	81.6	46.1	68.2
Ori-New	35.1	64.0	-	-	62.5	81.5	-	-

The results are shown in Table 6. On large-scale datasets, the accuracy of Asymmetric drops significantly. NCCL achieves better performance than baseline. Asymmetric is too local and restrictive to capture the intrinsic structure in the large datasets, while our method has a solid ability to obtain the intrinsic structure.

4.8. Discussion

Generally, three motivations drive us to deploy a new model: 1) growth in training data, 2) better model architecture, and 3) better loss functions. We have conducted detailed experiments on these three aspects. BCT can deal with the data growth and model architecture changes when the old and new training data have common classes. Asymmetric can handle data growth and model architecture changes well on small datasets, even better than BCT, but it is too local to work on large datasets reliably. Our method is the state-of-the-art under the changes of training data and model architectures. It achieves better cross-test performance and always gives better performance than the new model trained independently.

For loss functions, the change of embedding loss usually does not affect backward-compatible learning. In contrast, the change of classification loss will lead to both BCT failure, and Asymmetric failure, which means that the cross-test performance drops sharply or the new model’s performance is significantly damaged. However, our method can still improve the performance of the new model under the variation of classification loss. At the same time, the backward-compatible performance is obtained.

Table 7. Ablation study on Market1501. The new model is trained with 100 % Data using ResNet-18.

Methods	Self-Test			Cross-Test		
	R1	R5	mAP	R1	R5	mAP
Ori-Old(R18+50 %Data)	82.96	92.32	63.26	-	-	-
NCCL w/o neighborhood consensus	91.75	97.14	78.71	85.45	93.48	67.90
NCCL w/o pseudo-multi-label learning	91.98	97.48	80.08	85.51	94.83	68.40
NCCL w/o sample selection	92.58	97.30	80.18	85.05	95.07	68.72
NCCL	92.87	97.58	81.9	86.05	95.34	69.15
Ori-Old(R18+25 %Data)	70.13	86.07	46.42	-	-	-
NCCL w/o neighborhood consensus	91.81	97.09	79.40	76.63	91.57	55.60
NCCL w/o pseudo-multi-label learning	91.92	97.06	80.57	78.06	91.69	56.53
NCCL w/o sample selection	91.86	96.97	80.13	77.35	91.51	55.71
NCCL	92.64	97.24	81.41	78.06	91.98	57.44

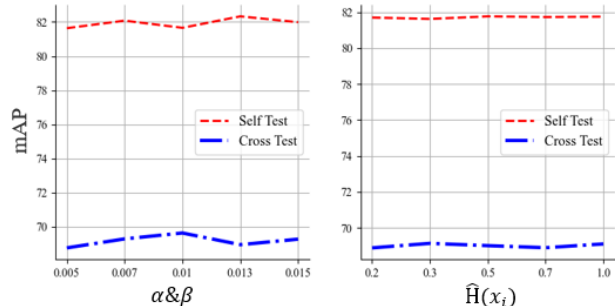


Figure 3. Performance under different $\alpha \& \beta$ and \hat{U} on Market1501. In the right part, the x -axis value represents $\hat{U} = x * \log K_{new}$.

4.9. Ablation study and Hyperparameter analysis

We test the effect of different modules in NCCL. As L_2 only works in the later stage of training, it need to work with L_1 . As is shown in Table 7, we can observe that adaptive neighborhood consensus helps to strengthen both self-test and cross-test performance significantly. The soft pseudo-multi-label learning also improves performance steadily but not as significant as the neighborhood consensus module. Besides, the proposed highly credible sample detection procedure does not bring significant performance up-gradation in all cases, which depends on the quality of the old model.

We also vary the three primary hyperparameters: α , β and \hat{U} . The α and β control the importance of the L_1 and L_2 , while \hat{U} is the uncertainty threshold for highly credible sample detection. For simplicity, we take $\alpha = \beta$ and change them from 0.005 to 0.015 and \hat{U} from $\frac{\log K_{new}}{5}$ to $\log K_{new}$. As is shown in Figure 3, our method is robust to these hyperparameters changes.

5. Conclusion

This paper proposes a neighborhood consensus contrastive learning framework with credible sample selection for feature compatible learning. We validate the effectiveness of our method by conducting thorough experiments in various reality scenarios using three ReID datasets and two large-scale retrieval datasets. Our method achieves the state-of-the-art performances and shows the convincing robustness in different case studies.

References

- [1] Song Bai, Peng Tang, Philip HS Torr, and Longin Jan Latecki. Re-ranking via metric fusion for object retrieval and person re-identification. *In Proceedings of the IEEE Conference on Computer Vision and Pattern Recognition*, pages 740–749, 2019.
- [2] Yan Bai, Yihang Lou, Feng Gao, Shiqi Wang, Yuwei Wu, and Ling-Yu Duan. Group-sensitive triplet embedding for vehicle reidentification. *IEEE Transactions on Multimedia*, 20(9):2385–2399, 2018.
- [3] Mateusz Budnik and Yannis Avrithis. Asymmetric metric learning for knowledge transfer. *arXiv preprint arXiv:2006.16331*, 2020.
- [4] Mathilde Caron, Ishan Misra, Julien Mairal, Priya Goyal, Piotr Bojanowski, and Armand Joulin. Unsupervised learning of visual features by contrasting cluster assignments. *In Thirty-fourth Conference on Neural Information Processing Systems*, 2020.
- [5] Dapeng Chen, Dan Xu, Hongsheng Li, Nicu Sebe, and Xiaogang Wang. Group consistent similarity learning via deep crf for person re-identification. *In Proceedings of the IEEE conference on computer vision and pattern recognition*, pages 8649–8658, 2018.
- [6] Ting Chen, Simon Kornblith, Mohammad Norouzi, and Geoffrey Hinton. A simple framework for contrastive learning of visual representations. *In International conference on machine learning*, pages 1597–1607, 2020.
- [7] Ting Chen, Simon Kornblith, Kevin Swersky, Mohammad Norouzi, and Geoffrey Hinton. Big self-supervised models are strong semi-supervised learners. *arXiv preprint arXiv:2006.10029*, 2020.
- [8] Xinlei Chen, Haoqi Fan, Ross Girshick, and Kaiming He. Improved baselines with momentum contrastive learning. *arXiv preprint arXiv:2003.04297*, 2020.
- [9] Ching-Yao Chuang, Joshua Robinson, Lin Yen-Chen, Antonio Torralba, and Stefanie Jegelka. Debaised contrastive learning. *arXiv preprint arXiv:2007.00224*, 2020.
- [10] Jia Deng, Wei Dong, Richard Socher, Li-Jia Li, Kai Li, and Li Fei-Fei. Imagenet: A large-scale hierarchical image database. *2009 IEEE conference on computer vision and pattern recognition*, pages 248–255, 2009.
- [11] Jiankang Deng, Jia Guo, Niannan Xue, and Stefanos Zafeiriou. Arcface: Additive angular margin loss for deep face recognition. *Proceedings of the IEEE Conference on Computer Vision and Pattern Recognition*, pages 4690–4699, 2019.
- [12] Yang Fu, Xiaoyang Wang, Yunchao Wei, and Thomas Huang. Sta: Spatial-temporal attention for large-scale video-based person re-identification. *In Proceedings of the AAAI conference on artificial intelligence*, 33(1):8287–8294, 2019.
- [13] Jean-Bastien Grill, Florian Strub, Florent Althé, Corentin Tallec, Pierre H Richemond, Elena Buchatskaya, Carl Doersch, Bernardo Avila Pires, Zhaohan Daniel Guo, Mohammad Gheshlaghi Azar, et al. Bootstrap your own latent: A new approach to self-supervised learning. *arXiv preprint arXiv:2006.07733*, 2020.
- [14] Yiluan Guo and Ngai-Man Cheung. Efficient and deep person re-identification using multi-level similarity. *In Proceedings of the IEEE Conference on Computer Vision and Pattern Recognition*, pages 2335–2344, 2018.
- [15] Kaiming He, Haoqi Fan, Yuxin Wu, Saining Xie, and Ross Girshick. Momentum contrast for unsupervised visual representation learning. *In Proceedings of the IEEE Conference on Computer Vision and Pattern Recognition*, pages 9729–9738, 2020.
- [16] Kaiming He, Xiangyu Zhang, Shaoqing Ren, and Jian Sun. Deep residual learning for image recognition. *Proceedings of the IEEE conference on computer vision and pattern recognition*, pages 770–778, 2016.
- [17] Lingxiao He, Xingyu Liao, Wu Liu, Xinchun Liu, Peng Cheng, and Tao Mei. Fastreid: A pytorch toolbox for general instance re-identification. *arXiv preprint arXiv:2006.02631*, 6(7):8, 2020.
- [18] Ruibing Hou, Bingpeng Ma, Hong Chang, Xinqian Gu, Shiguang Shan, and Xilin Chen. Vrsrc: Occlusion-free video person re-identification. *In Proceedings of the IEEE Conference on Computer Vision and Pattern Recognition*, pages 7183–7192, 2019.
- [19] Nakamasa Inoue and Keita Goto. Semi-supervised contrastive learning with generalized contrastive loss and its application to speaker recognition. *In 2020 Asia-Pacific Signal and Information Processing Association Annual Summit and Conference*, pages 1641–1646, 2020.
- [20] Sultan Daud Khan and Habib Ullah. A survey of advances in vision-based vehicle re-identification. *Computer Vision and Image Understanding*, 182:50–63, 2019.
- [21] Prannay Khosla, Piotr Teterwak, Chen Wang, Aaron Sarna, Yonglong Tian, Phillip Isola, Aaron Maschiot, Ce Liu, and Dilip Krishnan. Supervised contrastive learning. *arXiv preprint arXiv:2004.11362*, 2020.
- [22] Jianing Li, Jingdong Wang, Qi Tian, Wen Gao, and Shiliang Zhang. Global-local temporal representations for video person re-identification. *In Proceedings of the IEEE International Conference on Computer Vision*, pages 3958–3967, 2019.
- [23] Junnan Li, Pan Zhou, Caiming Xiong, Richard Socher, and Steven CH Hoi. Prototypical contrastive learning of unsupervised representations. *arXiv preprint arXiv:2005.04966*, 2020.
- [24] Xiao Liu, Fanjin Zhang, Zhenyu Hou, Zhaoyu Wang, Li Mian, Jing Zhang, and Jie Tang. Self-supervised learning: Generative or contrastive. *arXiv preprint arXiv:2006.08218*, 2020.
- [25] Aaron van den Oord, Yazhe Li, and Oriol Vinyals. Representation learning with contrastive predictive coding. *arXiv preprint arXiv:1807.03748*, 2018.
- [26] Xingang Pan, Ping Luo, Jianping Shi, and Xiaoou Tang. Two at once: Enhancing learning and generalization capacities via ibn-net. *Proceedings of the European Conference on Computer Vision*, pages 464–479, 2018.
- [27] Qi Qian, Lei Shang, Baigui Sun, Juhua Hu, Hao Li, and Rong Jin. Softtriple loss: Deep metric learning without triplet sampling. *Proceedings of the IEEE International Conference on Computer Vision*, pages 6450–6458, 2019.

- [28] Ruijie Quan, Xuanyi Dong, Yu Wu, Linchao Zhu, and Yi Yang. Auto-reid: Searching for a part-aware convnet for person re-identification. *In Proceedings of the IEEE International Conference on Computer Vision*, pages 3750–3759, 2019.
- [29] Filip Radenović, Ahmet Iscen, Giorgos Tolias, Yannis Avrithis, and Ondřej Chum. Revisiting oxford and paris: Large-scale image retrieval benchmarking. *In Proceedings of the IEEE Conference on Computer Vision and Pattern Recognition*, pages 5706–5715, 2018.
- [30] Yantao Shen, Yuanjun Xiong, Wei Xia, and Stefano Soatto. Towards backward-compatible representation learning. *In Proceedings of the IEEE Conference on Computer Vision and Pattern Recognition*, pages 6368–6377, 2020.
- [31] Yifan Sun, Changmao Cheng, Yuhan Zhang, Chi Zhang, Liang Zheng, Zhongdao Wang, and Yichen Wei. Circle loss: A unified perspective of pair similarity optimization. *Proceedings of the IEEE Conference on Computer Vision and Pattern Recognition*, pages 6398–6407, 2020.
- [32] Xun Wang, Xintong Han, Weilin Huang, Dengke Dong, and Matthew R Scott. Multi-similarity loss with general pair weighting for deep metric learning. *In Proceedings of the IEEE/CVF Conference on Computer Vision and Pattern Recognition*, pages 5022–5030, 2019.
- [33] Xudong Wang, Ziwei Liu, and Stella X Yu. Unsupervised feature learning by cross-level discrimination between instances and groups. *arXiv preprint arXiv:2008.03813*, 2020.
- [34] Yicheng Wang, Zhenzhong Chen, Feng Wu, and Gang Wang. Person re-identification with cascaded pairwise convolutions. *In Proceedings of the IEEE Conference on Computer Vision and Pattern Recognition*, pages 1470–1478, 2018.
- [35] Zhongdao Wang, Luming Tang, Xihui Liu, Zhuliang Yao, Shuai Yi, Jing Shao, Junjie Yan, Shengjin Wang, Hongsheng Li, and Xiaogang Wang. Orientation invariant feature embedding and spatial temporal regularization for vehicle re-identification. *Proceedings of the IEEE International Conference on Computer Vision*, pages 379–387, 2017.
- [36] Longhui Wei, Shiliang Zhang, Wen Gao, and Qi Tian. Person transfer gan to bridge domain gap for person re-identification. *Proceedings of the IEEE conference on computer vision and pattern recognition*, pages 79–88, 2018.
- [37] Nicolai Wojke and Alex Bewley. Deep cosine metric learning for person re-identification. *In 2018 IEEE winter conference on applications of computer vision*, pages 748–756, 2018.
- [38] Zhirong Wu, Yuanjun Xiong, Stella X Yu, and Dahua Lin. Unsupervised feature learning via non-parametric instance discrimination. *Proceedings of the IEEE Conference on Computer Vision and Pattern Recognition*, pages 3733–3742, 2018.
- [39] Hantao Yao, Shiliang Zhang, Richang Hong, Yongdong Zhang, Changsheng Xu, and Qi Tian. Deep representation learning with part loss for person re-identification. *IEEE Transactions on Image Processing*, 28(6):2860–2871, 2019.
- [40] Mang Ye, Chao Liang, Zheng Wang, Qingming Leng, and Jun Chen. Ranking optimization for person re-identification via similarity and dissimilarity. *In Proceedings of the 23rd ACM international conference on Multimedia*, pages 1239–1242, 2015.
- [41] Mang Ye, Jianbing Shen, Gaojie Lin, Tao Xiang, Ling Shao, and Steven CH Hoi. Deep learning for person re-identification: A survey and outlook. *IEEE Transactions on Pattern Analysis and Machine Intelligence*, 2021.
- [42] Hang Zhang, Chongruo Wu, Zhongyue Zhang, Yi Zhu, Zhi Zhang, Haibin Lin, Yue Sun, Tong He, Jonas Mueller, R Manmatha, et al. Resnest: Split-attention networks. *arXiv preprint arXiv:2004.08955*, 2020.
- [43] Yifan Zhang, Bryan Hooi, Dapeng Hu, Jian Liang, and Jiashi Feng. Unleashing the power of contrastive self-supervised visual models via contrast-regularized fine-tuning. *arXiv preprint arXiv:2102.06605*, 2021.
- [44] Liming Zhao, Xi Li, Yueting Zhuang, and Jingdong Wang. Deeply-learned part-aligned representations for person re-identification. *In Proceedings of the IEEE international conference on computer vision*, pages 3219–3228, 2017.
- [45] Liang Zheng, Liyue Shen, Lu Tian, Shengjin Wang, Jingdong Wang, and Qi Tian. Scalable person re-identification: A benchmark. *Proceedings of the IEEE international conference on computer vision*, pages 1116–1124, 2015.
- [46] Jincheng Zhong, Ximei Wang, Zhi Kou, Jianmin Wang, and Mingsheng Long. Bi-tuning of pre-trained representations. *arXiv preprint arXiv:2011.06182*, 2020.
- [47] Jincheng Zhong, Ximei Wang, Zhi Kou, Jianmin Wang, and Mingsheng Long. Bi-tuning of pre-trained representations. *arXiv preprint arXiv:2011.06182*, 2020.
- [48] Zhun Zhong, Liang Zheng, Zhiming Luo, Shaozi Li, and Yi Yang. Invariance matters: Exemplar memory for domain adaptive person re-identification. *In Proceedings of the IEEE Conference on Computer Vision and Pattern Recognition*, pages 598–607, 2019.
- [49] Bolei Zhou, Agata Lapedriza, Aditya Khosla, Aude Oliva, and Antonio Torralba. Places: A 10 million image database for scene recognition. *IEEE transactions on pattern analysis and machine intelligence*, 40(6):1452–1464, 2017.
- [50] Kaiyang Zhou, Yongxin Yang, Andrea Cavallaro, and Tao Xiang. Omni-scale feature learning for person re-identification. *In Proceedings of the IEEE International Conference on Computer Vision*, pages 3702–3712, 2019.